# Annealing of electron-, proton-, and ion-produced vacancies in Si

S. Dannefaer,[1] V. Avalos,[1] D. Kerr,[1] R. Poirier,[2] V. Shmarovoz,[3] and S. H. Zhang[4]
[1]*Department of Physics, University of Winnipeg, Winnipeg, Manitoba R3B 2E9, Canada*
[2]*Départément de Physique, Université de Montréal, Case Postale 6128 Succ. Centre-Ville, Montréal, Québéc H3C 3J7, Canada*
[3]*Joint Institute for Nuclear Research, Dubna, Russia*
[4]*Department of Materials Science, Lanzhou University, Lanzhou 730000, China*
(Received 5 May 2005; revised manuscript received 2 December 2005; published 10 March 2006)

Positron lifetime and Doppler measurements were performed on float-zone-refined and variously doped Czochralski-grown Si. The samples were irradiated by various particles ($e^-$, $p$, Kr) with energies between 2 MeV and 245 MeV. Electron or proton irradiation gave rise to divacancies, whereas the damage from ion implantation (Kr) was mainly in the form of four-vacancy clusters, with only a small fraction of vacancies in the form of divacancies. In the case of impurity-lean Si, detailed isothermal annealing at various temperatures between 125 °C and 500 °C showed that after an initial fast decrease in divacancy concentration, a much slower process of vacancy agglomeration took place. At 450 °C agglomeration steadily progressed even after 30 h of annealing at which point the average cluster size corresponded to ten monovacancies. In impurity-rich Si, containing oxygen and dopants, there is nearly no initial decrease in vacancy concentration, and isothermal and isochronal annealings showed that vacancy agglomeration was also nearly absent. Doppler data showed that vacancy-dopant complexes slowly acquired oxygen as annealing progressed, and these complexes survived annealing at 500 °C for many hours. Measurements between 8 K and 530 K on samples containing divacancies, or larger clusters, showed a temperature dependence of the positron trapping rate that cannot be explained by the clusters being negatively charged, but can be explained if neutral clusters have a weakly bound positron state which at low temperatures makes trapping more efficient. Generally, the present positron experiments have given an indication for the type of defects that survive annealing at temperatures where electron paramagnetic resonance and infrared spectroscopy yield little useful information.

DOI: 10.1103/PhysRevB.73.115202 PACS number(s): 61.72.−y, 61.80.−x, 78.70.−g

## I. INTRODUCTION

There is an enormous literature on the radiation damage of silicon, both theoretical and experimental, but there is scant experimental data on the subject of the agglomeration of vacancies and the factors that influence agglomeration. The exception is the divacancy ($V_2$) which has been thoroughly characterized by electron paramagnetic resonance[1,2] (EPR) when in its negatively or positively charged states and by correlation with infrared (IR) spectroscopy the EPR-inactive, but IR-active, neutral state of $V_2$ was associated with a wide optical absorption band peaking at 1.8 $\mu$m[3]. $V_2$ is stable at room temperature,[1] unlike the monovacancy, but at temperatures between 125 °C and 225 °C, depending (curiously) on the oxygen concentration, $V_2$ starts to disappear according to EPR,[1] deep-level transient spectroscopy,[4] and IR.[3] No new EPR spectra emerged as the divacancies disappeared,[2] and to the authors' knowledge no new IR absorption bands were identified to arise from vacancy agglomerates (Newman and Totterdell[5] searched in vain for such new absorption bands).

Physically, one would expect agglomeration of vacancies beyond $V_2$, but the lack of experimental evidence for this has stymied research into this particular aspect of defects in Si. Theoretical calculations,[6–8] on the other hand, all suggest that vacancy agglomeration beyond $V_2$ is energetically favorable and have identified clusters of particular stability such as hexavacancies. Recent data obtained by means of positron annihilation spectroscopy (PAS) on proton-irradiated Si (Ref. 9) conclusively showed that one of the annealing mechanisms of $V_2$ is, indeed, the formation of larger vacancy clusters.

This paper reports on the fate of irradiation-produced defects when annealed to temperatures beyond which EPR and IR signals have disappeared. Further experiments on 8-MeV proton-irradiated Si are reported here, and results from 2- or 8-MeV electron and 245-MeV ion (Kr) irradiations are also included. By using the same experimental technique to investigate a wide range of samples, which would have been impossible using EPR and IR and deep-level transient spectroscopy, we have aimed at obtaining a broad understanding of the production and, in particular, the annealing of irradiation-produced defects in silicon. One of the main results of this work is that divacancies in impurity-free Si gradually agglomerate to form vacancy clusters that are stable to at least 500 °C. Oxygen seriously interferes with this process by agglomerating at small vacancy clusters and preventing vacancy agglomeration. Another main result, but more so a positron annihilation issue, is that trapping of a positron at a neutral divacancy (and larger vacancy clusters) involves a weakly bound state.

## II. EXPERIMENT

### A. Irradiations and samples

The experimental conditions for the three types of irradiations were as follows: Protons had an energy of 8 MeV so that they penetrated the 0.3-mm-thick float-zone-refined Si

 

(Fz-Si) 7000–Ω cm samples. A flux of $2\times10^{15}$ cm$^{-2}$ h$^{-1}$ was administered for 21 h with the samples clamped to a Cu block cooled by liquid nitrogen; after irradiation, the samples were warmed to room temperature. Due to the depth of the *positron* implantation profile, two layers of 0.3-mm-thick samples were placed on either side of the positron source to ensure that all positrons annihilated inside the samples.

Electron irradiation at 2 MeV was done on the same type of Fz-Si as used in the proton irradiations and also on various doped Czochralski-grown Si (Cz-Si) samples using an energy of 8 MeV. The electron beam was pulsed (pulse length 3 $\mu$s, 240 pulses/s) and had a time averaged flux of $1\times10^{17}$ cm$^{-2}$ h$^{-1}$; during irradiation, the samples were cooled by water at 8 °C.

Ion implantation utilized 245-MeV Kr ions. The flux was $3.6\times10^{12}$ ions cm$^{-2}$ h$^{-1}$ and the 0.5-mm-thick samples were clamped on a Cu block at 30 °C during irradiation: The temperature of the implanted layer during irradiation was below 100 °C since subsequent annealing could be observed at 100 °C. The implanted samples were Cz-Si of *n*-type conductivity of 100 Ω cm ($\simeq10^{16}$ cm$^{-3}$ P) and with a concentration of $\simeq10^{18}$ cm$^{-3}$ interstitial oxygen. The penetration depth of the ions was 31 $\mu$m, which poses a slight experimental difficulty since only 27% of the positrons annihilate within the ion-implanted layer, while the remainder annihilate within the unimplanted part of the sample.

### B. Techniques

Optical absorption was done by standard Fourier-transform infrared spectroscopy (FTIR) in the wave number range of 2600–10 000 cm$^{-1}$ (0.322–1.24 eV), mostly at room temperature, but also as a function of temperature down to 6 K.

Positron lifetime spectra and Doppler broadened energy spectra of the 0.511-MeV annihilation $\gamma$ quanta were measured with equipment characterized by the following parameters: The three lifetime spectrometers had prompt time spectra of 180 ps, 200 ps, and 220 ps, and the Doppler equipment had an energy resolution of 1.2 keV (all numbers refer to the full width at half maximum of the respective resolution functions).

Each lifetime spectrum contained $1\times10^{7}$ counts accumulated with a count rate of typically 400 s$^{-1}$, except for low-temperature measurements, where the rate was 100–150 s$^{-1}$ due to the necessity of an increased detector separation. Positron source strengths varied between 15 and 20 $\mu$Ci and were encapsulated with 0.8-$\mu$m-thick Al foil. Each Doppler spectrum contained $2\times10^{6}$ counts within the annihilation peak, and lifetime as well as Doppler spectra were repeated 5 times to reduce, especially, the scatter between the lifetime parameters as calculated by the RESOLUTION program.[10] A source correction consisting of a 250-ps, 2.5% component was included in the analyses, but had an insignificant influence. Another source contribution of ~450 ps is sometimes encountered,[11] but was not observable in our case, likely due to the significantly weaker source strength compared to the 40–60 $\mu$Ci used in Ref. 11. Nevertheless, results were unaffected when assuming an additional lifetime of 450 ps with an intensity up to 2% in the source correction.

Positrons detect vacancies because their average electron density is less than in the perfect part—i.e., the bulk. In lifetime measurements this has the consequence of introducing a lifetime specific for the vacancy and longer than the bulk lifetime. In Doppler measurements the change in electron-momentum distribution caused by the vacancy is measured and is often parametrized by the $S$ parameter as defined in the following paragraph. The general expectation is that the lifetime of positrons increases with increasing size of vacancy agglomerates and that $S$ exhibits a similar trend.

Doppler data were analyzed in terms of the $S$ parameter, defined as the ratio between the number of counts in a narrow energy window (511±0.7 keV) centered at the peak of the bell shaped energy spectrum, and the number of counts in a wider energy range spanning the whole width of the spectrum (511±4.8 keV): In our case values of $S$ were close to 0.5, but no attempt was made to optimize this value along the lines described in Ref. 12.

Since lifetime spectra can be resolved into individual components, the trapping model[13] can be used to calculate the trapping rate of positrons by vacancies, a parameter which is proportional to the vacancy concentration and hence of physical importance. In the case of a single type of vacancies the trapping rate $\kappa$ is given by

$$\kappa = I_V(1/\tau_B - 1/\tau_V)/(1 - I_V). \tag{1}$$

In Eq. (1), $I_V$ is the experimentally determined intensity ($0 \leqslant I_V \leqslant 1$) of the lifetime component $\tau_V$ arising from positrons that annihilate in vacancies and $\tau_B$ is the lifetime of positrons determined in a Si sample which is free of positron traps (the so-called bulk lifetime). The subscript $V$ does *not* indicate a monovacancy, but simply a defect with vacancy character.

The experimentally measured Doppler parameter $S$ is in the case of a single vacancy type the weighted average of the $S$ parameters for positrons annihilating in the bulk ($S_{\mathrm{Ref}}$) and those trapped by vacancies ($S_V$); i.e., $S$ is

$$S = (1 - F)S_{\mathrm{Ref}} + FS_V. \tag{2}$$

$S_{\mathrm{Ref}}$ is the measure for (but not a determination of) the valence electron momentum distribution in the bulk; likewise for $S_V$, except that the distribution is changed locally at the vacancy and $S_V$ is usually larger than $S_{\mathrm{Ref}}$ The fraction of positrons that annihilate at vacancies, $F$, is according to the trapping model given by the expression

$$F = \kappa/(\kappa + 1/\tau_B), \tag{3}$$

where $\kappa$ is calculated from Eq. (1)—i.e., from *lifetime* data. $S$ and $S_{\mathrm{Ref}}$ are usually experimentally accessible, so with the (essential) help from lifetime data, the $S$ parameter characteristic of the defect ($S_V$) can be calculated. In this paper Doppler data will be presented in the convenient form of

$$\Delta S/S_{\mathrm{Ref}} = (S - S_{\mathrm{Ref}})/S_{\mathrm{Ref}}, \tag{4}$$

so that the expression for the defect specific value $\Delta S_V$ is

TABLE I. Characteristics of the unirradiated samples used in this work. Positron data were obtained at room temperature. The two resolvable lifetimes are denoted $\tau_1$ and $\tau_V$ with intensities of $I_1$ and $I_V$, respectively. The $\tau_1$ lifetime is slightly less than the bulk lifetime (218 ps) due to the weak presence of the $\tau_V$ lifetime. Doppler $S$ values are listed as $S_{\mathrm{Ref}}$, as they are used as reference values for the irradiated samples. In the last column is listed the radiation types used on the various samples.

| Sample No. | Sample type and doping | $\tau_1$ (ps) | $\tau_V$ (ps) | $I_1$ (%) | $I_V$ (%) | $S_{\mathrm{Ref}}$ ($\pm$0.0003) | Irradiation type |
|---|---|---|---|---|---|---|---|
| 1 | Fz, undoped $\sim$7000 $\Omega$ cm | 216±1 | 337±15 | 94±1 | 6±1 | 0.5082 | 8 MeV proton 2 MeV $e^-$ |
| 2 | Cz, P, $5\times10^{16}$ cm$^{-3}$ | 215±1 | 447±5 | 97±1 | 3±1 | 0.5065 | 245 MeV Kr |
| 3 | Cz, P, $5\times10^{18}$ cm$^{-3}$ | 210±2 | 360±10 | 93±0 | 7±1 | 0.5055 | 8 MeV $e^-$ |
| 4 | Cz, Sb, $1\times10^{18}$ cm$^{-3}$ | 212±2 | 365±20 | 94±2 | 6±2 | 0.5075 | 8 MeV $e^-$ |
| 5 | Cz, B, $5\times10^{18}$ cm$^{-3}$ | 210±2 | 380±30 | 98±2 | 2±2 | 0.5087 | 8 MeV $e^-$ |

$$\Delta S_V/S_{\mathrm{Ref}} = (\Delta S/S_{\mathrm{Ref}})/F, \tag{5}$$

where $\Delta S_V \equiv S_V - S_{\mathrm{Ref}}$. Equations (1)–(3) are the mathematics for a very simple physical scenario for positron annihilation—namely, that positrons have only two possibilities for annihilation, either in the bulk or in vacancies of the *same* type. This is rarely encountered, and a particularly cumbersome situation arises if the vacancy has a positron state whose binding energy is comparable to the thermal energy. Such a situation was considered theoretically[14] in the case of negatively charged vacancies and then applied to an analytical model[15] which vividly exhibits the convoluted way in which several physical parameters enter into the experimentally observed positron parameters.

## III. RESULTS

Positron data for the various Si samples used in the irradiation experiments are listed in Table I. Common to all of the samples was a contribution from grown-in vacancy clusters as shown by the $\tau_V$ lifetime component, but its intensity $I_V$ was low and essentially independent of the significant differences in impurity content and growth conditions among the various samples. The Doppler $S_{\mathrm{Ref}}$ parameter is slightly larger than the bulk value for $S$ due to the grown-in vacancy clusters: using the data in Table III, below, we estimate that $S_{\mathrm{Ref}}$ is larger than $S_B$ by 0.2%, a correction that we will disregard in this paper.

The results arising from the proton irradiated undoped Fz-Si constitute the backbone of this paper and are, therefore, presented in Sec. III A. The results from ion implantation are presented in Sec. III B, and Sec. III C contains results obtained from highly doped Cz-Si irradiated by 8-MeV electrons or by 2-MeV electron-irradiated Fz-Si.

### A. Proton irradiation

This section is divided into two parts, where the first (Sec. III A 1) deals with isothermal annealing and Sec. III A 2 with at-temperature measurements between 8 and 530 K.

#### 1. Isothermal annealing

Optical absorption spectra are shown in Fig. 1. The broad absorption band peaking at 6000 cm$^{-1}$ (1.67 $\mu$m at 6 K, 1.8 $\mu$m at 293 K) in panel (a) is due to neutral divacancies $V_2^0$ (Ref. 3) and the narrow peak at 2765 cm$^{-1}$ (3.6 $\mu$m) in panel (b) is due to $V_2^-$ (Ref. 16); the latter absorption is only observable below 150 K, but is an artifact arising from the white light used in FTIR. No other absorption bands were observed apart from the usual irradiation-produced featureless near band-edge absorption.

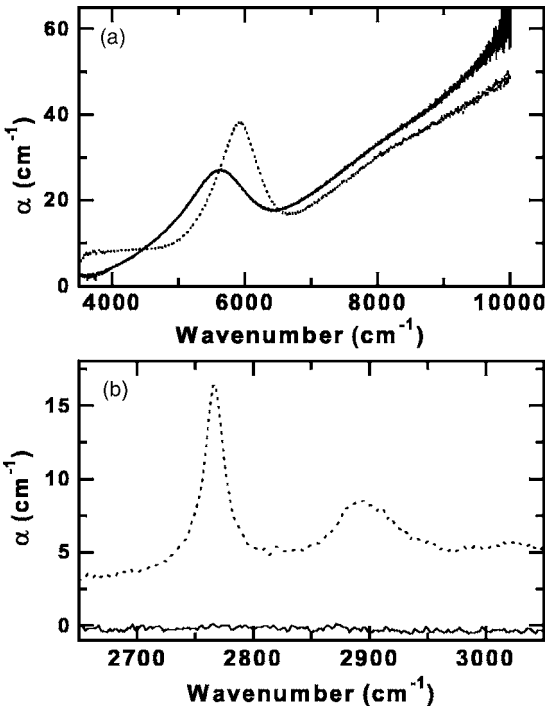


FIG. 1. Optical absorption coefficient for a proton irradiated sample (dose is $4\times10^{16}$ cm$^{-2}$) measured at 6 K (dashed lines) or at 293 K (solid lines). Absorption at $\sim$6000 cm$^{-1}$ in panel (a) is due to $V_2^0$ while $V_2^-$ gives rise to the two peaks shown in panel (b). These peaks become observable below 150 K.

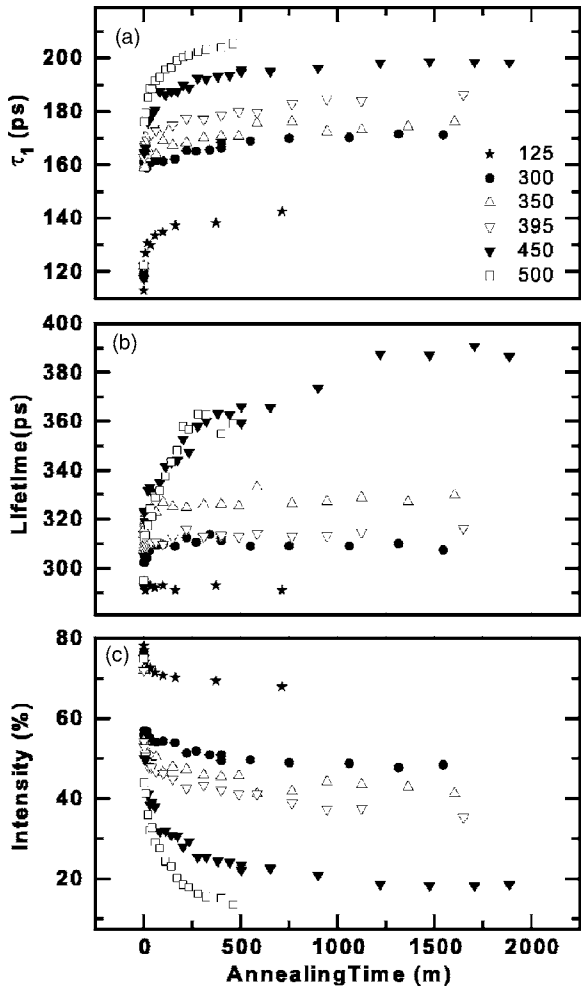


FIG. 2. Lifetime results obtained at 20 °C for proton irradiated Fz-Si at the various isothermal annealing temperatures (in °C) listed in panel (a). Panel (b) shows the time development of the irradiation-produced lifetime and panel (c) its intensity.

In Fig. 2 the data are shown for the two resolvable lifetime components as a function of isothermal annealing temperatures. The short-lived $\tau_1$ component is shown in panel (a), and its value is always smaller than the bulk lifetime (218 ps). In panel (b) is shown the second resolvable component, and its value is always larger than 218 ps. The intensity of this component is shown in panel (c), with the balance to 100% made up from the intensity of $\tau_1$. In Fig. 3 positron data are shown on an expanded time scale, to make visible data not obvious in Fig. 2.

Proton irradiation produced a lifetime of 292±2 ps [see Fig. 2(b) or 3(a)], and a like value was found after 2 MeV electron irradiation (300±5 ps),[9] 10 MeV electrons (305 ±10 ps),[17] and after 15 MeV electron irradiation of Fz-Si (295±5 ps).[18] These lifetimes were interpreted to arise from $V_2$, and calculations[19] support this interpretation. The trapping rates shown in Fig. 3(b) were calculated using the trapping model with the assumption of only one vacancy-associated positron state in addition to the bulk state [the case expressed by Eq. (1)], and the applicability thereof was tested, and confirmed, by the model, yielding a bulk lifetime

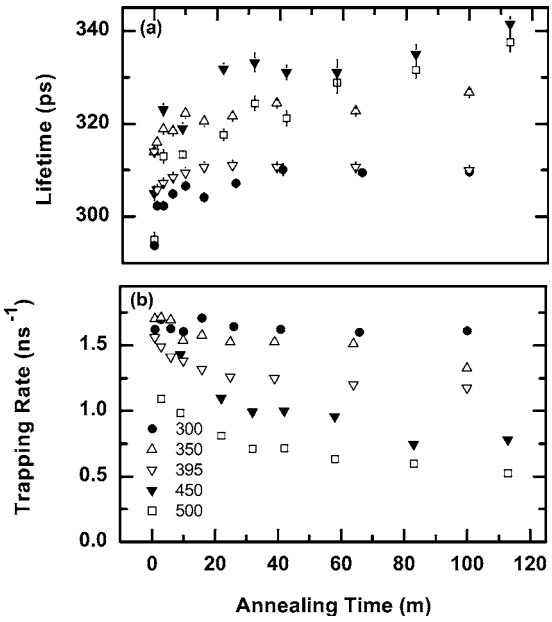


FIG. 3. Short-time annealing data which are not perceptible from the overview shown in Fig. 2. In panel (b) is shown the legend for the various annealing temperature in °C. Panel (a) shows the irradiation-produced lifetime and panel (b) the trapping rate as calculated from Eq. (1).

of 216–220 ps in agreement with experimental data (cf. Ref. 20 for details). In fact, for *all* of the lifetime data obtained at room temperature the model was adequate, but that was not the case for positron measurements below ~150 K, where the calculated values for $\tau_B$ increased gradually to 240 ps.

Positron lifetime data are shown in Figs. 2 and 3 for several isothermal annealing temperatures together with a result from annealing at 125 °C, published earlier[9] where isochronal annealing at 85 °C and at 100 °C also was investigated. The annealing data in Fig. 2(b) clearly show that depending on annealing temperature lifetimes ranging from 292 to 390 ps are approached. For annealing temperatures between 125 °C and 395 °C asymptotic values are obtained within less than 100 m (Fig. 3), but at 450 °C or at 500 °C, it is questionable if an asymptotic value is obtained even after 1800 m. Annealing at 500 °C was stopped already after 450 m due to the vacancy response becoming too small [10%, Fig. 2(c)] for an accurate determination of the positron lifetime.

The trapping rate decreases rapidly, within 1 min, from 4 ns$^{-1}$ to 1.5 ns$^{-1}$ for annealing temperatures above 125 °C, and is then followed by a *very* slow decrease. It is noted that within the first minute of annealing the positron lifetime increased only slightly, if at all, while the trapping rate decreased by *circa* 50% *independent of* annealing temperature between 300 °C and 500 °C. Two distinctly different processes are clearly at work in removing divacancies.

### *2. Temperature dependences*

Doppler broadening was used predominantly to investigate the temperature dependence of the trapping rate because Doppler experiments are sensitive to trapping rates of much

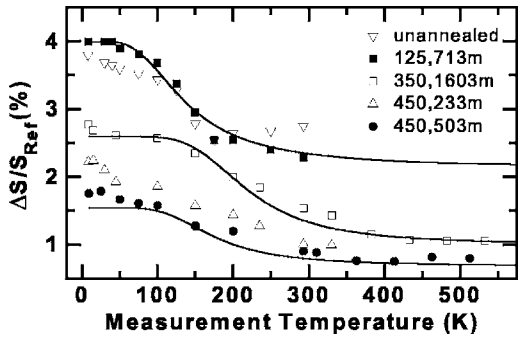


FIG. 4. Temperature dependencies of $\Delta S/S_{\mathrm{Ref}}$ for various annealings of proton irradiated Fz-Si. The legend shows the various annealing temperatures (in °C) and durations of annealing. The three curves are fits based on a model (Ref. 15) to be described in the Discussion, part B.

higher values than are lifetime measurements, although carefully chosen samples could be investigated by both techniques. Doppler data for an as-irradiated sample are shown in Fig. 4 together with data for various stages of annealings picked from the lifetime experiments shown in Fig. 2. $\Delta S/S_{\mathrm{Ref}}$ exhibits in all cases a sigmoidal change with sample temperature which will be discussed thoroughly.

The results for a sample that could be reliably investigated by lifetime spectroscopy are shown in Fig. 5. Of importance is that the defect's positron lifetime (358±5 ps) is independent of temperature and that calculating $\tau_B$ from the lifetime data using the trapping model[13] gave values that deviate significantly from the bulk lifetime of 218 ps below ~150 K, indicating that a different model is necessary at low temperatures.

### B. Ion implantation

Implantation by 245-MeV Kr ions was investigated in the dose range of $1\times10^{11}-1\times10^{13}$ ions cm$^{-2}$. Due to the fact that only ~27% of the positrons annihilate inside the implanted layer, the 73% contribution to lifetime and Doppler spectra coming from the unimplanted part of the sample

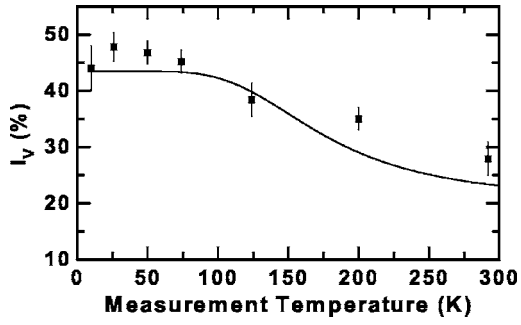


FIG. 5. Lifetime intensity as a function sample temperature for the sample that was proton irradiated and then annealed at 450 °C for 503 m. The lifetime $\tau_V$ was independent of temperature (360±20 ps). The same sample was used in the Doppler measurements giving results shown by the symbol (●) in Fig. 4. The curve is calculated from the model that was used to fit the experimentally independent Doppler data.

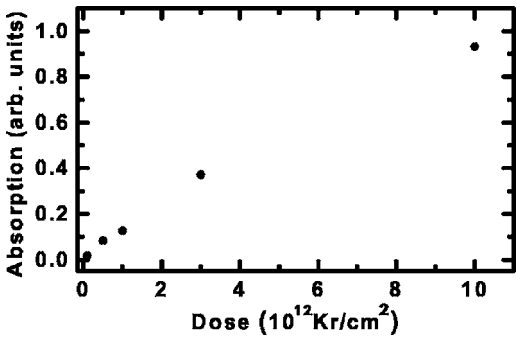


FIG. 6. Integrated optical absorption (between 5000 and 6250 cm$^{-1}$) measured at 293 K for $V_2^0$ as a function of Kr dose.

needs to be subtracted before analysis: Even though spectra for the unimplanted part of the sample were determined with an accuracy three times better than normally, lifetime and Doppler parameters pertinent to the implanted layer are intrinsically less well determined compared to the cases of proton and electron irradiation where the subtraction procedure is unnecessary.

As in the case of proton irradiation, infrared absorption at 1.8 $\mu$m (at room temperature) due to $V_2^0$ was measured for the Kr-implanted samples, but the absorption is weak because of the small thickness (31 $\mu$m) of the implanted layer. Integrated absorption between 1.6 $\mu$m and 2.0 $\mu$m *after* linear background correction is shown in Fig. 6 as a function of dose (the background correction is not trivial because it changes with dose due to the near band-edge absorption). $V_2^0$ is introduced linearly with dose, but as the positron data will show, divacancies are only a small part of the total inventory of vacancies.

In Fig. 7 are shown lifetime and Doppler data for a series of samples implanted by various doses of Kr. The positron lifetime is, to within experimental uncertainty, independent of dose (310±4 ps), and the trapping rate increases approximately linearly with dose to at least $3\times10^{12}$ cm$^{-2}$.

Isochronal annealing of the $1\times10^{11}$ and $1\times10^{13}$ cm$^{-2}$ irradiated samples was investigated by positrons giving the results shown in Fig. 8: Annealing between 100 °C and 200 °C is evident from the decrease in trapping rate [Fig. 8(b)], but vacancy clustering, as indicated by an increase in $\tau_V$, is obvious only for the heavily implanted sample.

Figure 9 shows the collected isochronal annealing data based on optical absorption at 1.8 $\mu$m after Kr implantation and after proton implantation[9] and the trapping rate from PAS: the responses are normalized to 1 before annealing to facilitate comparisons. The data clearly demonstrate a discrepancy between the annealing behavior as measured by optical absorption and by PAS.

Isothermal annealing at 450 °C, or at 500 °C, was also done on Kr-implanted Cz-Si samples (cf. Fig. 10) to facilitate comparison with proton-irradiated Fz-Si samples annealed at the same temperatures. For both types of irradiation the trapping rate decreases very rapidly within the first few minutes of annealing, but after that there is no evidence in Cz-Si for the gradual vacancy agglomeration seen in Fz-Si and annealing at 500 °C actually *reduces* the lifetime.

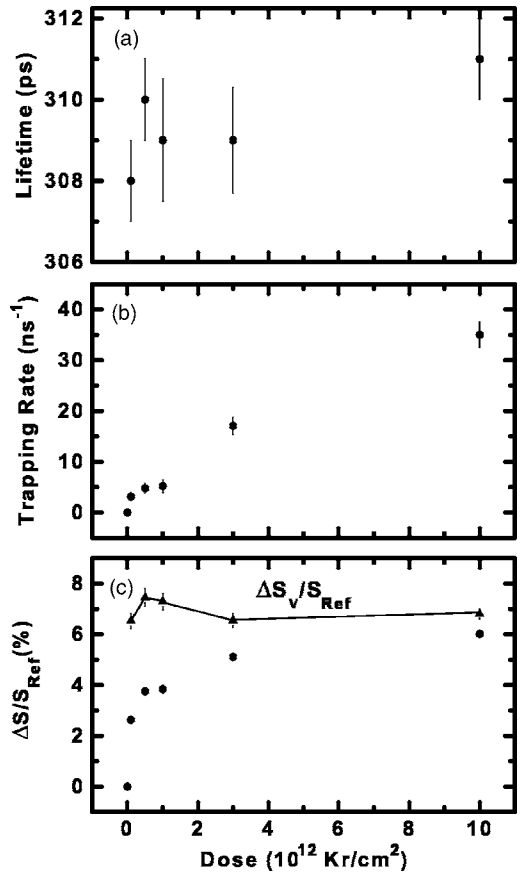


FIG. 7. Positron data obtained at 293 K as a function of ion dose. In panel (a) the lifetime produced by irradiation is shown and in panel (b) its trapping rate. Panel (c) shows in addition to $\Delta S/S_B$ (●) the values for the vacancy specific parameter (▲) $\Delta S_V/S_{\mathrm{Ref}}$ as calculated from Eq. (5).

### C. Electron irradiation

Electron irradiation at 2 MeV was done on undoped Fz-Si (the same wafer material as used for proton irradiation) and on heavily doped Cz-Si using 8-MeV electrons; cf. Table I. Electron irradiation had very diverse effects on the various samples, as listed in Table II. For example, in the case of undoped Fz-Si an accumulated dose of $6.4\times10^{18}\ e^-\ \mathrm{cm}^{-2}$ produced a weak response whereas it was very strong for the heavily doped samples.

A set of Fz-Si samples was investigated for several accumulated doses of 2-MeV electrons by means of Doppler broadening and lifetime spectroscopy. Figure 11 shows temperature dependences of $\Delta S/S_{\mathrm{Ref}}$ for three accumulated doses. The samples irradiated to the dose of $6.4\times10^{18}\ \mathrm{cm}^{-2}$ were also investigated by lifetime spectroscopy between 8 and 310 K, and the results are shown in Fig. 12. The curves shown in Figs. 11 and 12 are fits using the model that will be discussed in part B of the Discussion.

For the heavily doped Cz-Si samples only isochronal annealing was conducted and all of the positron measurements were done at room temperature. The annealing behaviors of P- (Fig. 13) and Sb- (Fig. 14) doped Cz-Si samples are similar: The trapping rate decreases monotonically over a wide temperature range, over which the positron lifetime shows small changes. In contrast to the small changes in lifetime $\Delta S_V/S_{\mathrm{Ref}}$ decreases from ~5% to ~1%, which is a significant decrease for a defect that gives essentially a constant positron lifetime. This suggests that the changes in the local

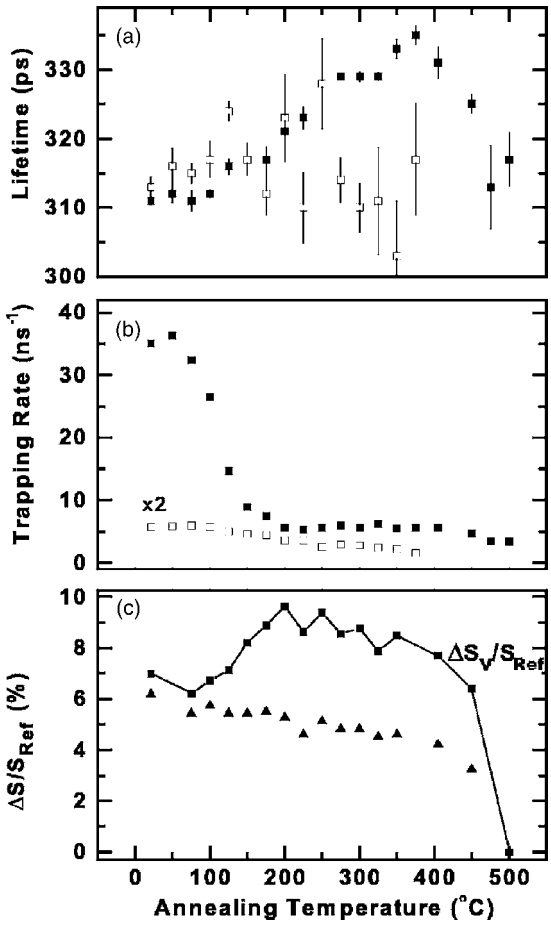


FIG. 8. Isochronal annealing $\left(\frac{1}{2}\ \mathrm{h}\right)$ of Kr-implanted Si as a function of annealing temperature. Two doses were investigated, $1\times10^{13}\ \mathrm{Kr\,cm}^{-2}$ (■) and $1\times10^{11}\ \mathrm{Kr\,cm}^{-2}$ (□). The Doppler data in panel (c) are for the $1\times10^{13}$ Kr dose only (▲), and the solid squares show $\Delta S_V/S_{\mathrm{Ref}}$ as calculated from Eq. (5). Measurements were done at 293 K.

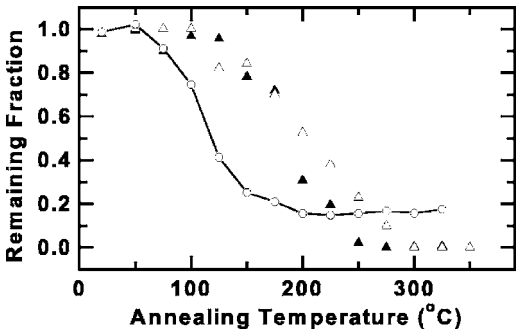


FIG. 9. Isochronal annealing $\left(\frac{1}{2}\ \mathrm{h}\right)$ of the optical absorption at 1.8 $\mu$m for $1\times10^{13}\ \mathrm{Kr\,cm}^{-2}$ (▲), $4\times10^{16}\ p\ \mathrm{cm}^{-2}$ (△), and the positron trapping rate shown in Fig. 8(b) for the $10^{13}$ Kr dose (○). Responses were normalized to 1 before annealing to facilitate comparisons. Measurements were done at 293 K.

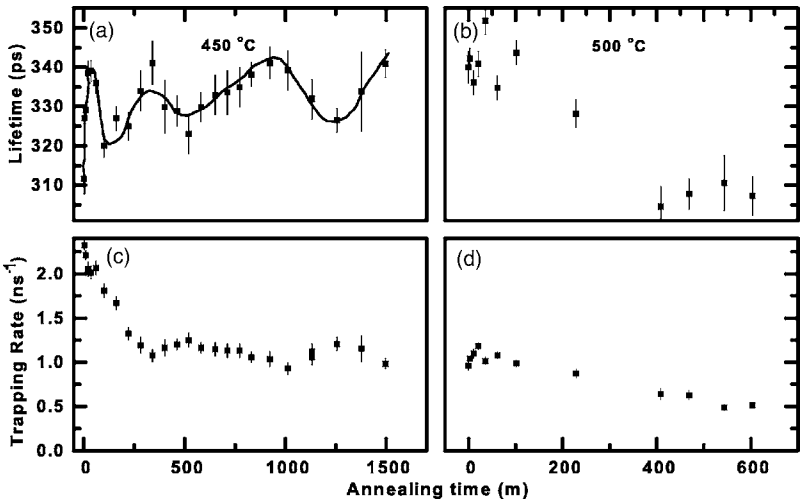


FIG. 10. Isothermal annealing data for a $3\times10^{12}$ Kr cm$^{-2}$ implanted sample annealed first at 450 °C [data shown in panels (a) and (c)] and subsequently at 500 °C [panels (b) and (d)]. Within the first minute of annealing at 450 °C the trapping rate decreased from 10 ns$^{-1}$ to 2.3 ns$^{-1}$, and 2.3 ns$^{-1}$ is the first data point shown in panel (c). Doppler data gave $\Delta S_V/S_{\mathrm{Ref}}=7\%$ before annealing and 0.2% at the end of the 450 °C annealing. The curve in panel (a) is shown to emphasize the oscillatory behavior of the lifetime arising from the vacancy distribution. Annealing at 500 °C was stopped after 600 m due to the response from the implanted layer becoming too small for reliable analysis even for lifetime spectra containing $6\times10^7$ counts. Positron measurements were done at 293 K.

electron momentum distribution, revealed by $\Delta S_V/S_{\mathrm{Ref}}$, and in the local electron density, revealed by the lifetime, are not trivially correlated. This is also evident in the case of the B-doped Cz-Si (Fig. 15) where vacancy agglomeration takes place during annealing, but $\Delta S_V/S_{\mathrm{Ref}}$ nevertheless decreases; a decrease (from 7% to 0.2%) was also observed in Kr-implanted low-doped Cz-Si during annealing at 450 °C. In Table III are collated $\Delta S_V/S_{\mathrm{Ref}}$ values and lifetimes for various samples and annealings.

## IV. DISCUSSION

There are two parts to the discussion: In the first part (A) defect characterization is the main topic, while in the second (B) positron issues arising from the temperature dependences of the positron parameters are discussed.

### A. Defect characterization

It is relevant first to consider what the value of the positron lifetime might be for $V_2$. The reason is that theoretical calculations[19] indicate that the increment in positron lifetime per added vacancy is only about 10 ps, so positron lifetimes must be known very accurately if they are to be used for assessing the size of the vacancy clusters, and $V_2$ is the fundamental cluster. One theoretical calculation for neutral $V_2$ (Ref. 19) gave values between 298 ps and 309 ps dependent on whether relaxation of the divacancy was not taken into account (former value) or was. In another calculation[7] unrelaxed $V_2$ gave a lifetime of 303 ps, but relaxation reduced the value to 240 ps. Yet another calculation[21] gave a positron lifetime of 302 ps which was reduced to 280 ps upon relaxation, and a recent work[8] gave 296 ps before relaxation and 255 ps after relaxation. The various theoretical calculations agree very well when relaxation is *not* taken into account (296–303 ps), and they also agree with the experimental values claimed to arise from $V_2$ (295–325 ps), but the reductions in lifetime[7,8,21] due to relaxation are unrealistic since they result in lifetimes smaller than for monovacancies: There are obvious problems with the theoretical treatment of relaxation, except in the case of the approach in Ref. 19, for which reason we compare our experimental results with this particular work.

In this paper the lifetime for the neutral $V_2$ is taken to be $297\pm2$ ps based on results from 10-MeV electron-irradiated Fz-Si,[17] 2-MeV electron-irradiated Fz-Si (this work), and 8-MeV proton-irradiated Fz-Si (this work and Ref. 9). The value is at the very bottom of the experimental lifetime range of 300–330 ps (Refs. 22–29), ascribed to $V_2$ for neutron or proton irradiated Si (Fz or Cz) for a wide range of particle energies (1–65 MeV), so for these cases contributions from

TABLE II. Positron results after irradiation of the sample types listed in Table I. In all cases an irradiation-produced lifetime could be observed, denoted by $\tau_V$ and with intensity $I_V$. The trapping rate $\kappa_V$ is calculated from Eq. (1). The Doppler response is $\Delta S/S_{\mathrm{Ref}}$. In the last column doses and particle-type are listed. All data are obtained at room temperature.

| Sample No. | $\tau_V$ (ps) | $I_V$ (%) | $\kappa_V$ (ns$^{-1}$) | $\Delta S/S_{\mathrm{Ref}}$ (%) | Dose (cm$^{-2}$) |
|---|---|---|---|---|---|
| 1 | 290±3 | 81±1 | 4.9±0.2 | 2.6 | $4\times10^{16}$ $p$ |
| 1 | 295±5 | 15±2 | 0.2±0.02 | 0.4 | $6.4\times10^{18}$ $e^-$ |
| 2 | 310±2 | 78±1.5 | 4.8±0.5 | 4.0 | $5\times10^{11}$ Kr |
| 3 | 240±3 | 95±0.5 | 12±2 | 3.3 | $0.8\times10^{18}$ $e^-$ |
| 4 | 270±2 | 90±1 | 14±4 | 4.4 | $0.8\times10^{18}$ $e^-$ |
| 5 | 301±2 | 68±1 | 2.8±0.3 | 2.8 | $0.8\times10^{18}$ $e^-$ |

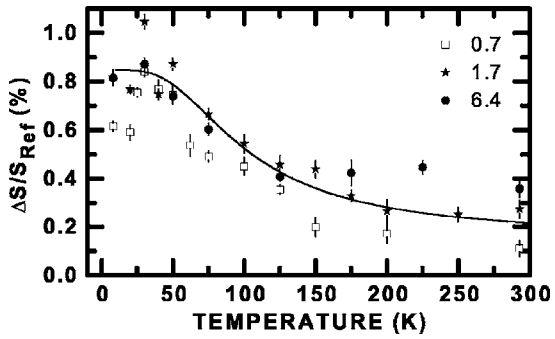


FIG. 11. Doppler data as a function of sample (undoped Fz-Si) temperature for various accumulated doses of 2-MeV electrons. In the legend, doses are in units of $10^{18}$ $e$ cm$^{-2}$. The curve is a fit to the data for the highest dose and is generated from the best fit to the experimentally *independent lifetime* data shown in Fig. 12 (fitting parameters are shown in Table V).

larger clusters are likely the cause for the experimentally observed lifetimes.

The isothermal annealing experiments shown in Figs. 2 and 3 were done to investigate the time development of vacancy concentration *and* vacancy agglomeration at various temperatures (proton decoration of vacancies can be ruled out because protons were not implanted into the samples). The very fast decrease (within 1 m) of the trapping rate without any change in lifetime indicates, as also suggested by annealings at 85, 100, and 125 °C,[9] that interstitials are the source for the fast removal of vacancies. The fact that nearly the same fraction of $V_2$ (close to 50%) is removed *regardless* of annealing temperature between 125 °C and 500 °C indicates that most of the interstitials are released to recombine with $V_2$ at 125 °C, and the activation energy was estimated to be 1.0±0.1 eV.[9]

The process of vacancy clustering is not analyzable in terms of simple kinematics since it is a multistep process. However, the positron data indicate that vacancies form stable cluster configurations at 300, 350, and 395 °C, and they are apparently infrared inactive, as also supported by a recent theoretical work,[8] and they have not been reported on using EPR. From PAS there is finally the experimental evidence for what happens to $V_2$ during annealing in Fz-Si; i.e., close to 50% of the divacancies are removed by interstitials, and the rest slowly agglomerates.

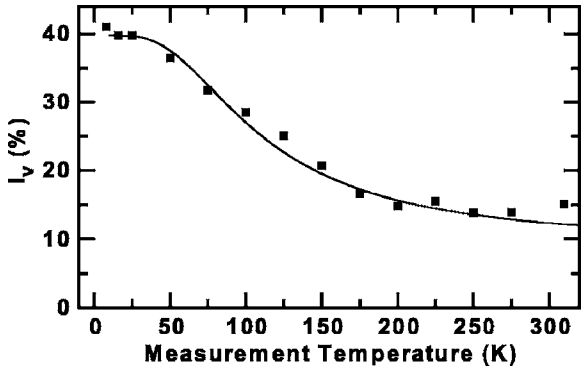


FIG. 12. Lifetime results for the undoped Fz-Si sample irradiated with 2-MeV electrons to an accumulated dose of 6.4 $\times 10^{18}$ cm$^{-2}$. The lifetime was fixed at 295 ps since it showed no variation with temperature. The curve is generated from the model using the parameter values listed in Table V. The same parameter values were used to fit the $\Delta S/S_B$ data in Fig. 11.

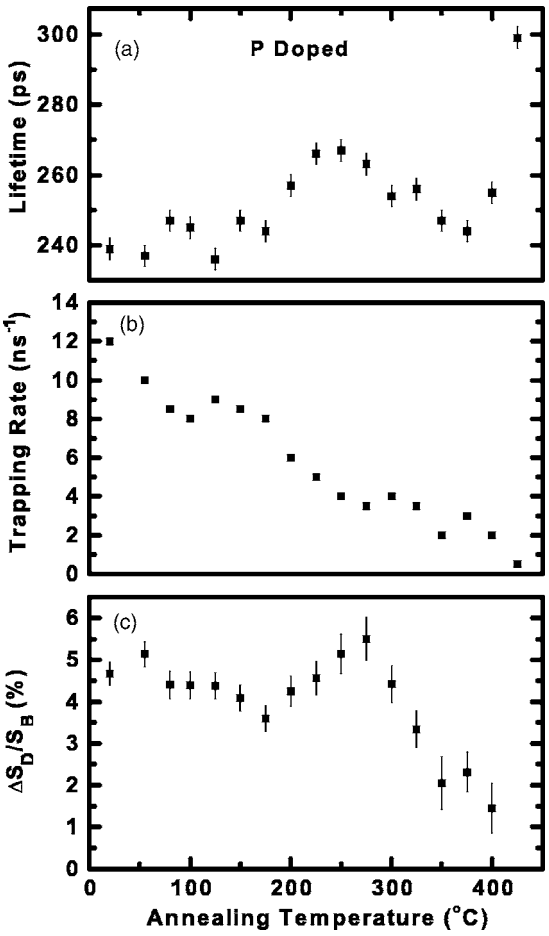


FIG. 13. Isochronal $\left(\frac{1}{2}\text{ h}\right)$ annealing of 8-MeV electron-irradiated heavily P-doped ($5\times 10^{18}$ cm$^{-3}$) Cz-Si. The irradiation-produced lifetime is shown in panel (a), its trapping rate in panel (b), and in panel (c) the defect-specific $\Delta S_V/S_{\text{Ref}}$ is shown as calculated from Eq. (5). Positron measurements were done at 293 K.

Annealing below 395 °C is low enough for stable lifetimes whose values according to theory correspond to $V_4$ clusters; see Table IV. This is a reasonable result arising from migration of $V_2$ that does not involve dissociation of $V_2$.[30] The ~20 ps difference in lifetime after long annealing times at 350 °C or at 395 °C can possibly be ascribed to different configurations of the four-vacancy agglomerate. Increasing the isothermal annealing temperature to 450 °C exceeds the thermal stability of $V_4$ vacancy clusters, causing continuing growth. However, during growth there might be formed some clusters that are particularly stable, and hence last longer, and that would create a plateau for the lifetime. This is observed (cf. Fig. 3) where the lifetime is constant at 332±4 ps for annealing between 20 and 90 min, and could, according to Table IV, arise from $V_4$. Essentially, this indicates that $V_4$ is a particularly stable, although not the most stable vacancy configuration: Another plateau in the increase

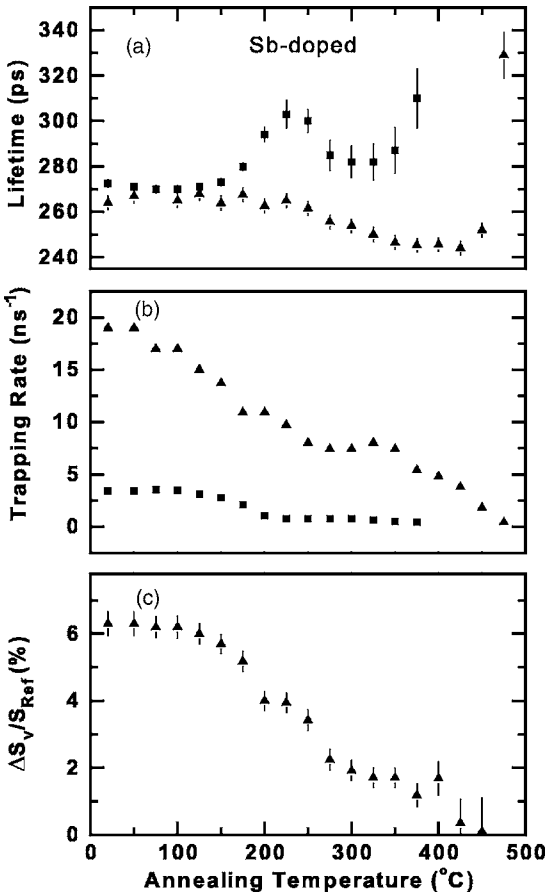


FIG. 14. Isochronal $(\frac{1}{2}\ \mathrm{h})$ annealing of electron irradiated Sb-doped $(1\times10^{18}\ \mathrm{cm}^{-2})$ Cz-Si. Two irradiation doses were investigated, one being $3\times10^{17}\ \mathrm{cm}^{-2}$ at 2–3 MeV, the other being $1\times10^{18}\ \mathrm{cm}^{-2}$ at 8 MeV. Squares in the panels refer to the low-energy case and triangles to the high-energy case. Positron measurements were done at 293 K. The panels depict the same parameters as in Fig. 13.

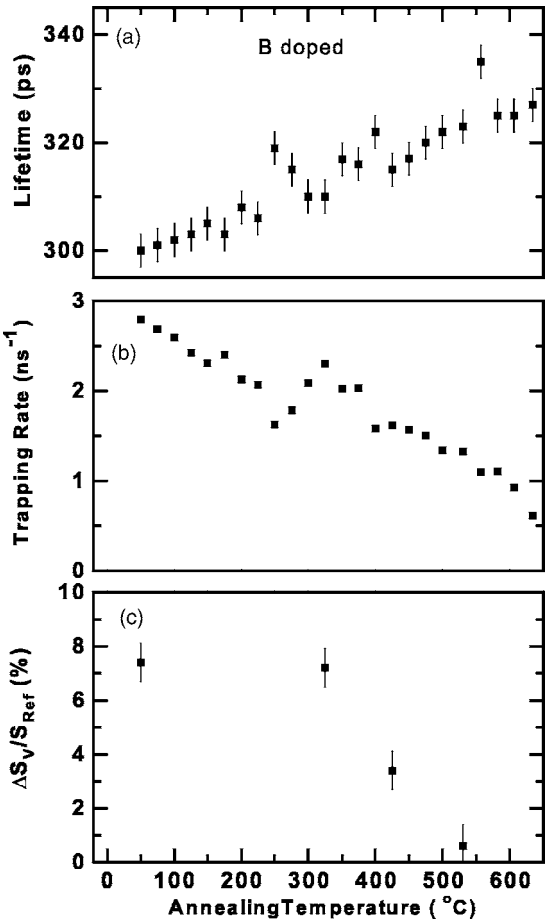


FIG. 15. Isochronal $(\frac{1}{2}\ \mathrm{h})$ annealing of electron irradiated heavily B-doped $(5\times10^{18}\ \mathrm{cm}^{-3})$ Cz-Si. Positron measurements were done at 293 K, and the panels depict the same parameters as in Fig. 13.

of $\tau_2$ occurs at ~360 ps after annealing between 400 and 700 m at 450 °C. This lifetime is characteristic of $V_6$,[19] which is another particularly stable vacancy agglomerate. Vacancy clusters in Fz-Si created by annealing at 450 °C for 30 h have an average size of ten vacancies according to Ref. 19. These clusters are not stable in view of results on Fz-Si plastically deformed at room temperature:[31] Vacancy clusters were formed that gave rise to a positron lifetime of 460 ps which was unaffected by annealing to ~800 °C for $\frac{1}{2}$ h, and the lifetime suggests an *average* size of 18 vacancies, nearly twice that found in this work.

In the case of ion implantation vacancy clusters larger than $V_2$ are expected and that is indeed confirmed by the 310±2 ps lifetime [Fig. 7(a)] indicative of $V_4$. In a work similar to ours, Kr implantation gave rise to a lifetime of 303±1 ps.[32] In Fig. 8(b), the decrease in the trapping rate near 100 °C indicates again that interstitials are the source for the fast removal of these vacancies. However, not all of the vacancies are in the form of $V_4$; there are also $V_2$. In the temperature interval (~150–300 °C) where *all* of the optical absorption due to $V_2$ disappears (Fig. 9) the positron response decreases by only ~10%; i.e., *some 90% of the vacancy clusters seen by positrons are invisible to IR*: That PAS and IR observe different vacancy-type defects is also evident by comparing the trapping rate [Fig. 7(b)] with the IR absorption (Fig. 6) as a function of dose, where at low doses the PAS response increases much faster than does the IR response.

In contrast to the case of proton irradiation, Kr is implanted into the sample, which raises the possibility of implant-vacancy reactions either during implantation or during annealing. Traditionally, damage due to ions has been investigated using slow positron beams (see, for example, Refs. 33 and 34) due to the damaged layer being a few micrometers thick. Here, the damaged layer is 27 $\mu$m thick (as in Ref. 32), so the experimental situation is quite different. For example, within the straggling depth for the Kr ions (1 $\mu$m according to TRIM), only 2.5% of the positrons that annihilate in the 27-$\mu$m-thick damaged layer arise from the 1-$\mu$m-thick Kr containing layer.

During annealing at 450 °C, or 500 °C, Kr conceivably could diffuse and decorate vacancies, although the temperature appears low compared to the 300 °C necessary for making $V_2$-He complexes[34] and ~800 °C for making bubbles after Ne implantation.[35] At any rate, the implanted Kr would give a concentration of only $10^{15}\ \mathrm{cm}^{-3}$ if spread evenly over

TABLE III. Summary of lifetime and Doppler data obtained from as-irradiated and annealed samples. All measurements were made at room temperature. The first five rows pertain to unannealed samples, while the following rows are for annealed samples. In the third column, the parameter $\Delta\tau_V$ is $(\tau_V - \tau_B)$.

| Defect lifetime $\tau_V$ (±3 ps) | $\Delta S_V/S_{\mathrm{Ref}}$ (%) (±0.3%) | $(\Delta S_V/S_{\mathrm{Ref}})/(\Delta\tau_V/\tau_B)$ (±0.03) | Comments |
|---|---|---|---|
| 240 | 4.5 | 0.45 | Unannealed P-doped Cz-Si (Fig. 13) |
| 270 | 6.2 | 0.26 | Unannealed Sb-doped Cz-Si (Fig. 14) |
| 295 | 6.0 | 0.17 | Unannealed Fz-Si; based on data in Figs. 2 and 4 |
| 300 | 7.5 | 0.20 | Unannealed B-doped Cz-Si (Fig. 15) |
| 310 | 7.0 | 0.17 | Unannealed Fz-Si (Fig. 7) |
| 330 | 7.0 | 0.14 | Annealed Fz-Si (350 °C, 1602 m): based on data in Figs. 2 and 4 |
| 360 | 8.2 | 0.13 | Annealed Fz-Si (450 °C, 503 m): based on data in Figs. 2 and 4 |
| 255 | 0 | 0 | Sb-doped Cz-Si annealed to 420 °C (Fig. 14) |
| 255 | 1.5 | 0 | P-doped Cz-Si annealed to 400 °C (Fig. 13) |
| 310 | 0 | 0 | P-doped Cz-Si annealed to 500 °C (Fig. 10) |
| 325 | 0 | 0 | B-doped Cz-Si annealed to 525 °C (Fig. 15) |

the whole of the damaged layer, which is at least two orders of magnitude less than the vacancy concentration. Hence, the only impurity that materially can interfere with vacancies is oxygen.

It is striking that damage arising from a very wide range of particles and energies results in a very narrow range of lifetimes (297–310 ps), which indicates a modest range in cluster size of $V_2$–$V_4$. In particular the apparent lack of large vacancy clusters in the 245-MeV Kr-irradiated samples is surprising and may indicate that large vacancy clusters are surrounded by $V_2/V_4$ complexes which trap positrons before they manage to detect the larger clusters. The oscillations in lifetime with annealing time at 450 °C [Fig. 10(a)] are not observed using 8-MeV proton irradiation and originate possibly from fluctuations in vacancy size in regions containing a large concentration.

TABLE IV. Lifetimes for proton-irradiated Fz-Si after long annealing times at various temperatures.

| Annealing temperature (°C) | $\tau_V$ (ps) | Cluster size[a] |
|---|---|---|
| ≤125 | 295±3 | $V_2$ |
| 300 | 305±5 | $V_2+V_4$ |
| 350 | 330±3 | $V_4$ |
| 395 | 310±3 | $V_4$ |

[a]Reference 19.

Impurities influence significantly the types of defects created *during* irradiation. In P- and Sb-doped samples the lifetime was 240–270 ps (Figs. 13 and 14), indicating that P (or Sb) traps mobile monovacancies. The lifetime for the Sb-vacancy complex is significantly larger than the calculated value of 234 ps (Ref. 36) for Sb-$V$, but for the P-$V$ complex there is very good agreement. Part of the reason for the discrepancy might arise from a Sb-$V_2$ contribution which would give a (calculated) lifetime of 294 ps (Ref. 36). However, it should be noted that no relaxations were incorporated in the calculations, and Ref. 19 clearly shows that such should be incorporated. In the case of B-doped samples the nearly pure divacancy response (300 ps, Fig. 15) is due to the fact that the boron-monovacancy complex is not stable at room temperature.[37] In addition to dopants, interstitial oxygen atoms also trap monovacancies, whereupon substitutional oxygen is formed ($A$ centers), but these centers could not be detected optically due to saturation of absorption arising from doping. These defects are not detected by PAS at room temperature,[38] but are a potential source of migrating oxygen above 250 °C where they disappear.[39]

We now turn to the role of impurities on the *annealing* of irradiation-produced vacancies. Although the detailed annealing patterns vary between the different impurities, the important observation is that there is no evidence for the

vacancy agglomeration that was observed in impurity-free Fz-Si. Impurities clearly are traps for vacancies, but simple dopant-vacancy complexes (the *E* centers observed by EPR) are not the traps beyond ~150 °C due to their thermal instability.[40] Traps stable at higher temperatures may consist of several dopant atoms somehow agglomerated to surround a monovacancy as in the case of heavily As-doped Si (Ref. 36) or by impurity-divacancy complexes created during the breakup of *E* centers: The latter possibility would explain the transient increase in lifetime above 150 °C as shown in Figs. 13 and 14. However, such an explanation is not viable in the case of Kr-implanted P-doped Cz-Si since the P concentration is too small ($5\times10^{16}$ cm$^{-3}$) for multi-dopant-vacancy complexes to be formed at a concentration sufficient to account for the trapping rates shown in Figs. 8 and 10. Oxygen is, therefore, the impurity common to all Cz-type samples that prevents the vacancy agglomeration observed in Fz-Si, and the experimental evidence for oxygen decoration of vacancies comes from the Doppler data shown in Fig. 8 for annealing temperatures above 400 °C, Table III, and Figs. 13–15: $\Delta S_V/S_{\mathrm{Ref}}$ decreases well below the value for divacancies [~6% (Ref. 17) and from Table III, third row], but this decrease is not accompanied by a decrease in lifetime. Oxygen atoms surrounding a vacancy (be it a monovacancy, a divacancy, etc.) are expected to reduce $\Delta S_V/S_{\mathrm{Ref}}$ because the outer electrons of oxygen have higher momenta than do those of Si. In the case of oxygen its effect on the valence electron momentum distribution immediate to the vacancy is so large that one does not have to resort to the more difficult type of measurements that look for the impurity influence via the weakly detected core electrons. In Ref. 41, oxygen was inferred to stabilize vacancies and the convincing evidence from this work, as well as from Refs. 11 and 42, is that during annealing $S_V$ decreases to a value close to $S_{\mathrm{Ref}}$.

The agglomeration of oxygen around vacancy clusters also explains the gradual decrease in positron lifetime upon annealing at 500 °C [Fig. 10(c)]. The absence thereof during annealing at 450 °C (at least for 1500 m) indicates that within a 50 °C temperature interval there occurs a significant change in the morphology of the vacancy-oxygen cluster. It is in this temperature range that thermal donors are generated, and we speculate that they originate from oxygen agglomerated around a vacancy.

### B. Positron issues

Several works on Fz-Si,[17,22,43–45] together with the present one, have indicated a significant temperature dependence of the trapping rate which varies by roughly a factor of 10 between 10 and 293 K. At low temperatures theory predicts a $T^{-1/2}$ dependence and that was observed experimentally in the 10–60-K temperature range:[43–45] At higher temperatures theory predicts a much stronger temperature dependence and is experimentally observed as a $T^{-n}$ dependence ($n$ ~1.5–3) in the 200–300-K temperature range. There are, however, experimental works that indicate much different temperature dependences. In one work[46] the trapping rate exhibits a temperature dependence that suggests negatively charged vacancies, but at 35 K there is a peak that certainly cannot be explained by a $T^{-1/2}$ dependence. Significantly, EPR and IR data gave no indication for the presence of $V_2^-$, so the authors suggested a model involving resonance trapping by *neutral* $V_2$. Another work,[28] reporting on 1-MeV neutron-irradiated Fz-Si, leads to the conclusion that the intensity of the lifetime arising from $V_2$ *increases* with temperature, whereas the opposite was found here as well as in the above-mentioned works. The temperature dependence of positron trapping seems to be heavily influenced by extraneous effects arising from impurities and the Fermi level.

The temperature dependences found in this work are all characterized by a nearly temperature-independent response below ~100 K (cf. Figs. 4, 5, and 11). Very similar temperatures dependences of the Doppler *S* parameter were reported in Ref. 32 on Kr-implanted Si. The $T^{-1/2}$ dependence is obviously ruled out, and it is most unlikely that additional positron traps active only below ~100 K (so-called shallow traps) play any role: Such traps would only weakly localize the positron wave function for which reason lifetime and Doppler parameters would be close to bulk values, causing $\Delta S/S_{\mathrm{Ref}}$ and the observed lifetime to decrease. That not being the case rules out shallow traps.

In a recent work[47] it was suggested that the $T^{-1/2}$ dependence at temperatures below 20 K would be modified due to the positrons not being fully thermalized, the consequence being that below ~20 K the trapping rate becomes nearly independent of temperature for negatively charged divacancies. The present data exhibit a similar effect, but in a significantly wider temperature range 8–100 K, and at higher temperatures the trapping decreases much slower than $T^{-n}$ ($n>1.5$), which is characteristic for negatively charged divacancies. Incomplete thermalization may take place, but the consequences thereof are not important in our case, and the reason, we believe, is that the vacancies are neutral—i.e., do not possess the near continuum of shallow so-called Rydberg states specific to negatively charged vacancies.

To explain the data we suggest that positrons trapped by neutral divacancies are trapped either directly from the bulk or via a vacancy-associated shallow state which may be viewed as an excited positron state at the vacancy. This model is conceptually like the one suggested for $V_2^-$,[48] where the Coulomb field arising from negatively charged $V_2$ introduces the shallow states. For the sake of easy reference a pictorial of the model from Ref. 15 is reproduced in Fig. 16, but with notation altered to remove reference to the shallow Rydberg state specific to the Coulomb field. Positrons occupy initially only the bulk state (upper heavy horizontal line) from where they may either annihilate by the rate $\lambda_B$ or be trapped into the shallow state, where they can annihilate by the rate $\lambda_B$, or from the vacancy where they annihilate by the rate $\lambda_V$. The specific trapping rates $\mu_{BS}$, $\mu_{BV}$, and $\eta_{SV}$ are defined in Fig. 16 and are assumed temperature independent, so $\mu_{SB}$ is the *sole* temperature-dependent parameter since it involves thermally activated detrapping.

Table V lists the various parameters used to obtain the fits shown in Figs. 4, 5, 11, 12, and 17. In column 2, the defect positron lifetime is listed for each of the samples, and values for the defect-specific $\Delta S_V/S_{\mathrm{Ref}}$ were calculated from Eq. (5). These parameters were obtained from room temperature measurements and by using the simple trapping model, be-

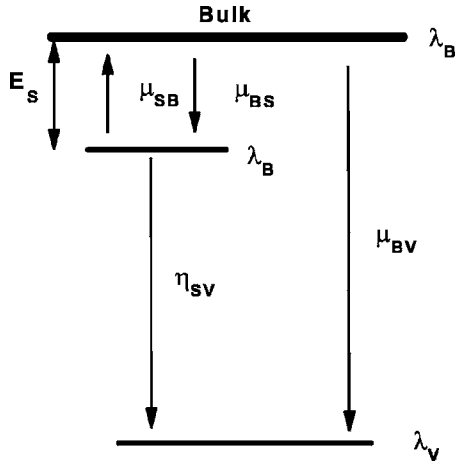


FIG. 16. A model for positron trapping at a defect that involves a positron state intermediate between the bulk state and the vacancy state. The parameters used in this figure are the same as used in Table V. The intermediate (shallow) state is situated at an energy $E_S$ below the bulk state and is comparable to thermal energy at 300 K, whereas the vacancy state is much deeper. The arrows indicate transitions between the three positron states; the lowest-energy state is the positron trapped in the vacancy giving rise to the annihilation rate $\lambda_V = 1/\tau_V$.

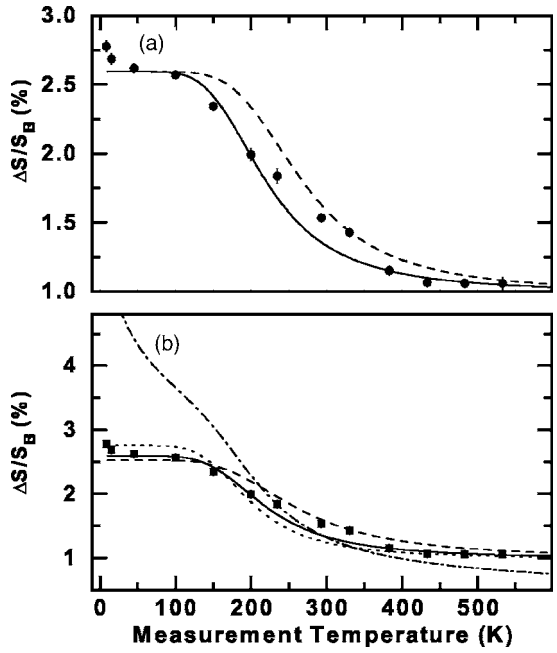


FIG. 17. Various fits to the experimental data for proton irradiated Fz-Si annealed at 350 °C for 1603 m using the model of Ref. 15; the parameters bracketing the experimental data are listed in Table V, last three columns in the second row. In panel (a) only $E_S$ was varied, whereas in (b) only $\mu_{BS}$ and $\eta_{SV}$ were varied. The consequence of assuming a $T^{1/2}$ dependence of the trapping rate pertinent for negatively charged $V_2$ is shown in panel (b) by the dash-dotted curve.

cause at that temperature effects from the shallow positron state are small, albeit not entirely absent as is evident from the tail-like behavior of $\Delta S/S_{\mathrm{Ref}}$ (cf. Fig. 17) between 300 °C and 530 °C. The defect concentration listed in the third column is based on the value assumed for $\mu_{BV}$, since it is the *product* of vacancy concentration and $\mu_{BV}$ that determines the defect trapping rate within the framework of the simple trapping model. The two specific trapping rates $\mu_{BS}$ and $\eta_{SV}$ are expected to be strongly correlated when fitting the experimental data since they govern the overall trapping into the defect via the shallow state; $E_S$ determines the temperature region in which the change in $\Delta S/S_{\mathrm{Ref}}$ takes place.

There are, to our knowledge, no theoretical estimates for the values of $\mu_{BS}$, $\eta_{SV}$, and $E_S$, so it is particularly important to investigate the range of parameter values that can produce acceptable fits (no elaborate $\chi^2$ analysis was done since that requires more data points). As an example, we analyzed the Doppler data for the samples annealed at 350 °C for 1603 m. Figure 17 shows acceptable fits to the data using the range of parameter values listed in Table V, second row ($\mu_{BV}$ was kept constant at $0.5\times10^{15}$ s$^{-1}$, a value normally employed for neutral vacancies[38]). We include in Fig. 17 the

TABLE V. Values of the parameters used in the model depicted in Fig. 16 to fit Doppler data (Fig. 4) for proton-irradiated Fz-Si samples (first three rows), annealed at various temperatures and times, and those used to fit the *electron*-irradiated samples (last row). The electron dose was $6.4\times10^{18}$ $e^-$ cm$^{-2}$, and the fit is shown in Fig. 11. This fit, however, was based on a fit to the lifetime parameter $I_V$ shown in Fig. 12.

| Sample | $\tau_V$ (ps) | $\Delta S_V/S_{\mathrm{Ref}}$ (%) | $C_V$ (ppm) | $\mu_{BV}$ ($\times10^{15}$ s$^{-1}$) | $\mu_{BS}$ ($\times10^{15}$ s$^{-1}$) | $\eta_{SV}$ ($\times10^{9}$ s$^{-1}$) | $E_S$ (meV) |
|---|---|---|---|---|---|---|---|
| Annealed 125 °C, 713 m | 295 | 6.0 | 25 | 0.5 | 6 | 13 | 20 |
| Annealed 350 °C, 1603 m | 304 | 7.0 | 7.5 | 0.5 | 7 or 2 | 5 or 14 | 60 or 80 |
| Annealed 450 °C, 503 m[a] | 360 | 8.2 | 4.1 | 0.5 | 1.7 | 6 | 40 |
| Unannealed *e*-irr | 295 | 6.0 | 1.2 | 0.5 | 3.0 | 40 | 10 |

[a]The fit to the experimentally independent lifetime parameter $I_V$ is shown in Fig. 5 using the above listed parameter values.

effect that a $T^{-1/2}$ dependence of $\mu_{BV}$ and $\mu_{BS}$ would have—i.e., if the vacancies were negatively charged. Rates associated with the shallow state could be varied, but only by a factor of 2 on either side of the best-fit values, and $E_S$, the depth of the shallow state, could be modestly varied between 60 and 80 meV.

Notwithstanding the daunting number of parameters in the model, their "orthogonality" nevertheless results in a reasonably accurate determination of their values. Values for $\mu_{BS}$ are definitely larger than for $\mu_{BV}$, which is ascribed to the small energy dissipation during shallow trapping, where only a couple of optical phonons need to be emitted during the trapping process: As to $\eta_{SV}$, its values express the rate by which a positron deexcites from a highly excited state (here referred to as the shallow state) to the ground state. The rates are at least an order of magnitude larger than for photon-mediated transitions, so phonon-mediated deexcitation dominates.

In closing this discussion we consider two issues. The first was pointed out in Ref. 49—namely, that there is an empirical relation between $\Delta S_V/S_{\mathrm{Ref}}$ and $\Delta\tau_V/\tau_B$ such that their ratio is close to 0.18. In Table III further values are listed, and they support the above-mentioned value, except in the case of P-doped Cz-Si, but here the influence from impurities may be particularly pronounced, as they are in the case of oxygen where the ratio is close to zero.

The second issue is an estimate for the specific trapping rate for vacancy clusters larger than $V_2$. For this estimate it is assumed that vacancies are not lost during agglomeration after the fast annealing step where vacancies indeed are lost. The assumption is in the present case of Fz-Si a good approximation, since the vacancy cluster concentration is much higher than the impurity concentration. We use the lifetime data for the 450 °C isothermal annealing since these data exhibit the widest span in lifetimes (cf. Figs. 2 and 3). The trapping rate in the case of divacancies is $\kappa_{2V}=\mu_{2V}C_{2V}$, where $C_{2V}$ is the concentration of divacancies and $\mu_{2V}$ the trapping rate per unit concentration (i.e., the specific trapping rate). Likewise, for clusters containing $n$ vacancies $\kappa_{nV}=\mu_{nV}C_{nV}$, so from the assumption of no loss of vacancies it follows that

$$\frac{\mu_{nV}}{\mu_{2V}}=\frac{n}{2}\frac{\kappa_{nV}}{\kappa_{2V}}. \tag{6}$$

Since the experimental data for annealing at 450 °C reflect a *distribution* of cluster sizes, $n$ in Eq. (6) means an average size, and using the theoretical correlation between lifetime and cluster size,[19] the experimentally measured lifetime yields the average value of $n$. According to Fig. 18, $\mu_{nV}/\mu_{2V}$ is independent of (average) $n$ values between 3 and 10, indicating that geometrical size is not of importance, although it does become of importance for much larger clusters.[50] The result is of practical interest since it permits an estimate for cluster concentrations for small clusters.

Finally, we again[51] point out the possibility that positrons may alter the charge of vacancies at low temperature. During slowdown of positrons from an average kinetic energy of 300 keV electron-hole pairs are created and that makes charging of vacancies possible at low temperatures where electronic equilibrium may not be achieved. Light with energy larger than the band gap causes this effect as demonstrated by photo-EPR (Ref. 1) and is demonstrated here by the presence of the 2765-$\mathrm{cm}^{-1}$ [3.6-$\mu$m] band [cf. Fig. 1(b)] observable below 150 K.

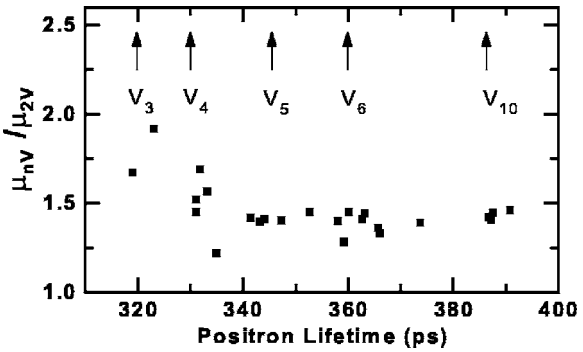


FIG. 18. Ratio between the specific trapping rate for vacancy clusters larger than divacancies ($\mu_{nV}$) and that for divacancies ($\mu_{2V}$). The data are obtained from the experimental data for proton irradiated Fz-Si annealed for various times at 450 °C (Figs. 2 and 3). Theoretical (Ref. 19) lifetimes for various clusters are indicated by arrows.

## V. CONCLUSION

Vacancies created by 2-MeV electron or by 8-MeV proton irradiation survive at room temperature as divacancies provided the absence of vacancy traps. Irradiation by 245-MeV Kr ions gives rise to vacancy clusters with an average size of four monovacancies and only ~10% of the clusters are in the form of divacancies.

Isothermal annealing of Fz-Si at various temperatures indicates that divacancies are removed by two mechanisms. The first is due to recombination with mobile interstitials and close to 50% of the vacancies are removed independently of annealing temperatures between 125 °C and 500 °C. The second annealing mechanism arises from a very slow agglomeration of vacancies which at temperatures at or below 395 °C produces stable (at least for 30 h) vacancy clusters consisting of four monovacancies. At 450 °C these clusters become unstable and agglomeration continues reaching an average of ~10 monovacancies after 30 h. The positron results provide the experimental evidence that vacancy agglomeration is a process intrinsic to pure Si.

Impurities severely modify the intrinsic process of vacancy agglomeration. In the case of Cz-Si the oxygen impurity, and not the various dopants, stabilizes vacancies to temperatures as high as 600 °C and oxygen is gradually being precipitated around vacancies during hour-long isothermal annealing at 450 °C/500 °C.

The temperature dependence of positron trapping is explained by a model which invokes a weakly bound positron state in addition to direct trapping, resulting in a temperature dependence distinct from that arising from negatively charged vacancies. In the range of vacancy clusters containing between three and ten vacancies (average values) the specific trapping rate is constant and 50% larger than for divacancies.

**ACKNOWLEDGMENTS**

This work was supported in part by the Natural Sciences and Engineering Research Council of Canada and by the National Research Council at Ottawa through their provision of electron irradiation, for which we are particularly grateful to Dr. C. Ross. We also acknowledge work done by P. Potrebko and S. Conci.

[1] G. D. Watkins and J. W. Corbett, Phys. Rev. **138**, A543 (1965).
[2] J. W. Corbett and G. D. Watkins, Phys. Rev. **138**, A555 (1965).
[3] L. J. Cheng, J. C. Corelli, J. W. Corbett, and G. D. Watkins, Phys. Rev. **152**, 761 (1966).
[4] For a recent summary, see V. P. Markevich, A. R. Peaker, S. B. Lastovskii, L. I. Murin, and L. J. Lindström, J. Phys.: Condens. Matter **15**, 2779 (2003).
[5] R. C. Newman and D. H. J. Totterdell, J. Phys. C **8**, 3944 (1975).
[6] N. Cuendet, T. Halicioglu, and W. A. Tiller, Appl. Phys. Lett. **67**, 1063 (1995).
[7] T. E. M. Staab, A. Sieck, M. Haugk, M. J. Puska, Th. Frauenheim, and H. S. Leipner, Phys. Rev. B **65**, 115210 (2002).
[8] D. V. Makhov and Laurent J. Lewis, Phys. Rev. Lett. **92**, 255504 (2004).
[9] R. Poirier, V. Avalos, S. Dannefaer, F. Schiettekatte, and S. Rooda, Physica B **340-342**, 609 (2003).
[10] P. Kirkegaard, N. J. Petersen, and M. Eldrup, computer code PAFIT-88, Risø M-2740, Risø, DK-4000 Roskilde, Denmark.
[11] H. Kauppinen, C. Corbel, J. Nissilä, K. Saarinen, and P. Hautojärvi, Phys. Rev. B **57**, 12911 (1998).
[12] X. D. Pi, C. P. Burrows, and P. G. Coleman, Appl. Surf. Sci. **194**, 255 (2002).
[13] R. N. West, Adv. Phys. **22**, 263 (1973).
[14] M. J. Puska, C. Corbel, and R. M. Nieminen, Phys. Rev. B **41**, 9980 (1990).
[15] S. Dannefaer and A. Pu, Nucl. Instrum. Methods Phys. Res. A **462**, 596 (2001).
[16] F. Carton-Merlet, B. Pajot, D. T. Don, C. Porte, B. Clerjaud, and P. M. Mooney, J. Phys. C **15**, 2239 (1982).
[17] V. Avalos and S. Dannefaer, Phys. Rev. B **54**, 1724 (1996).
[18] A. Kawasuso, M. Hasagawa, M. Suezawa, S. Yamaguchi, and K. Sumino, Jpn. J. Appl. Phys., Part 1 **34**, 2197 (1995).
[19] M. Saito and A. Oshiyama, Phys. Rev. B **53**, 7810 (1996).
[20] A. Pu, T. Bretagnon, D. Kerr, and S. Dannefaer, Diamond Relat. Mater. **9**, 1450 (2000).
[21] J. Kuriplach, A. L. Morales, C. Dauwe, D. Segers, and M. Šob, Phys. Rev. B **58**, 10475 (1998).
[22] S. Dannefaer, G. W. Dean, D. P. Kerr, and B. G. Hogg, Phys. Rev. B **14**, 2709 (1976).
[23] R. Oshima, M. Mori, G.-C. Jua, S. Honda, M. Kiritani, and F. E. Fujita, Mater. Sci. Forum **38-41**, 1199 (1989).
[24] A. Uedono, Y.-K. Cho, S. Tanigawa, and A. Ikari, Jpn. J. Appl. Phys., Part 1 **33**, 1 (1994).
[25] H. Maorong, W. Yunyu, Y. Juhua, H. E. Yonshu, G. Yinhyan, and L. Caichi, Chin. Sci. Bull. **42**, 26 (1997).
[26] H. Kauppinen, C. Corbel, K. Skog, K. Saarinen, T. Laine, P. Hautojärvi, P. Desgardin, and E. Ntsoenzok, Phys. Rev. B **55**, 9598 (1997).
[27] M. Coeck, M. Balcaen, T. van Hoecke, B. van Waeyenberge, D. Segers, C. Dauwe, and C. Laermans, J. Appl. Phys. **87**, 3674 (2000).
[28] V. Bondarenko, R. Krause-Rehberg, H. Feick, and C. Davia, J. Mater. Sci. **39**, 919 (2004).
[29] S. Dannefaer, P. Mascher, and D. Kerr, J. Appl. Phys. **73**, 3740 (1993).
[30] G. S. Hwang and William A. Goddard III, Phys. Rev. B **65**, 233205 (2002).
[31] H. S. Leipner, Z. Wang, H. Gu, V. V. Mikhnovich, Jr., V. Bondarenko, R. Krause-Rehberg, J.-L. Demont, and J. Rabier, Phys. Status Solidi A **201**, 2021 (2004).
[32] L. Liszkay, K. Havancsák, and Zs. Kajcsos, Appl. Surf. Sci. **149**, 181 (1999).
[33] P. J. Simpson, M. Vos, I. V. Mitchell, C. Wu, and P. J. Schultz, Phys. Rev. B **44**, 12180 (1991).
[34] M. Fujinami, T. Miyagoe, T. Sawada, R. Suzuki, T. Ohdaira, and T. Akahane, Phys. Rev. B **68**, 165332 (2003).
[35] E. Oliviero, S. Peripolli, P. F. P. Fichter, and L. Amaral, Mater. Sci. Eng., B **112**, 111 (2004).
[36] V. Ranki, A. Pelli, and K. Saarinen, Phys. Rev. B **69**, 115205 (2004).
[37] G. D. Watkins, Phys. Rev. B **13**, 2511 (1976).
[38] P. Mascher, S. Dannefaer, and D. Kerr, Phys. Rev. B **40**, 11764 (1989).
[39] B. G. Svensson and L. L. Lindström, Phys. Rev. B **34**, 8709 (1986).
[40] A. Nylandsted Larsen, J. J. Goubet, P. Mejlholm, J. Sherman Christensen, M. Fanciulli, H. P. Gunnlaugsson, G. Weyer, J. Wulff Petersen, A. Resende, M. Kaukonen, R. Jones, S. Öberg, P. R. Briddon, B. G. Svensson, J. L. Lindström, and S. Dannefaer, Phys. Rev. B **62**, 4535 (2000).
[41] A. Polity, F. Börner, S. Huth, S. Eichler, and R. Krause-Rehberg, Phys. Rev. B **58**, 10363 (1998).
[42] R. S. Brusa, W. Deng, G. P. Karwasz, A. Zecca, and D. Pliszka, Appl. Phys. Lett. **79**, 1492 (2001).
[43] S. Dannefaer, S. Kupca, B. G. Hogg, and D. P. Kerr, Phys. Rev. B **22**, 6135 (1980).
[44] J. Mäkinen, C. Corbel, P. Hautojärvi, P. Moser, and F. Pierre, Phys. Rev. B **39**, 10162 (1989).
[45] J. Mäkinen, P. Hautojärvi, and C. Corbel, J. Phys.: Condens. Matter **4**, 5137 (1992).
[46] A. Kawasuso and S. Okada, Jpn. J. Appl. Phys., Part 1 **36**, 605 (1997).
[47] J. Nissilä, K. Saarinen, and P. Hautojärvi, Phys. Rev. B **63**, 165202 (2002).
[48] M. J. Puska, C. Corbel, and R. M. Nieminen, Phys. Rev. B **41**, 9980 (1990).
[49] S. Dannefaer and D. Kerr, Diamond Relat. Mater. **13**, 157 (2004).
[50] S. Dannefaer, P. Mascher, and D. Kerr, J. Appl. Phys. **69**, 4080 (1991).
[51] S. Dannefaer and V. Avalos, Phys. Rev. B **60**, 1729 (1999).